

Optics and Device Simulation of Surface Plasmonic Enhancement of Organic Solar Cell Performance using Silver Nano-Prisms

Wenjun Jiang

Department of Physics
University of Washington
wjjiang@uw.edu

Michael Salvador

Department of Chemistry
University of Washington

David S. Ginger

Department of Chemistry
University of Washington

Scott T. Dunham

Department of Electrical Engineering
University of Washington
Seattle, WA 98195, United States
dunham@ee.washington.edu

Abstract—We explore the enhancement of light absorption due to triangular silver nano-prisms in polymer active layer and its impact on organic solar cell performance by coupling optical and electronic device simulation. We use optics simulation via FDTD solution of Maxwell's equations (Lumerical[®]) in order to calculate the plasmon resonance at the interface of polymer and silver nano-prisms. The silver nano-prisms result in dramatic local enhancement of optical absorption. We explore different design of silver nano-prisms by changing sizes, densities, and relative orientations to see their impact on optical generation. From the device modeling point of view, a thinner active layer enabled by enhanced absorption reduces the mismatch of light absorption depth with exciton dissociation length. We use the Sentaurus Device simulator (Synopsys[®]), adapted with material-specific models for electronic polymers, to explore the impact of plasmonic resonance on device behavior. The coupling of optics and device simulation gives larger short-circuit current and maximum power density for the thickness of P3HT:PCBM being less than 60nm. This simulation framework serves as baseline for designing polymer-based solar cells that can achieve the desired goal of 15% efficiency.

Keywords—organic solar cell; surface plasmonic effect; modeling; exciton dissociation

I. INTRODUCTION (HEADING 1)

Organic solar cells of nanostructures have been proposed as potential alternatives of conventional photovoltaics due to higher charge collection efficiency, newer power conversion mechanism, and lower cost.

Since it was first demonstrated that organic materials could be used to conduct electrons, many efforts have been concentrated on using organic materials to absorb sunlight. Three main types of organic photovoltaic devices (OPV) have been developed, that is, single layer OPV, double layered OPV, and heterojunction OPV.²⁻⁴ In February 2012, researchers in Polyera Inc. achieved a record efficiency of 9.1%.⁵ However, at least 15% efficiency needs to be achieved to beat silicon-based solar cells from the cost point of view.⁶ Many process, optical,

and device engineering techniques have been used to absorb more light in organic active layers by properly designing back metal reflector⁷ and reducing the recombination rate by controlling the phase-separation morphology of heterojunctions.⁸

Recent advances in nanotechnology allow materials to be fabricated and characterized on the nanoscale,^{9,10} which enable researchers to control the properties of materials to reveal new aspects of science and to find new applications. Surface plasmons are of great interest to many research areas ranging from physics, materials science and chemistry to biology. Silver nanoparticles are of particular interest due to high conductivity, localized surface plasmon resonance (LSPR) tunability, and thickness of adjacent materials precisely. For example, surface plasmons are under research for their promising potential in transformational optics,¹¹ magneto-optics,¹² optical sensors,¹³ light-emitting diodes,¹⁴ and solar cells.¹⁵

The use of localized surface plasmonic resonances as a means to absorb more light in solar cells is currently a hot research topic in organic photovoltaics due to LSPRs' ability to enhance near-field electron oscillation and eventually light absorption dramatically. Many different designs of metal nanoparticles have been studied such as core-shell structure¹⁶ and nano-disk array.¹⁷ In this paper, we analyzed silver nanoprisms as their sharp corners can enhance localized surface plasmon polaritons oscillations dramatically. We used finite-difference time-domain (FDTD) solution of Maxwell's equations to compare different sizes, shapes, and adjacent material choices for silver nanoprisms that are used to more effectively couple sunlight into P3HT:PCBM layer. Our optical calculation result shows good match with Professor David Ginger's experimental results,¹ and our device simulation predicts 3 times larger short-circuit current for 35nm active layer compared to system without nanoprisms.

II. OPTICS SIMULATION

A. FDTD calculation procedure

We used finite-difference time domain (FDTD) modeling to numerically compute the absorption enhancement that is induced by placing a triangular silver nanoprism inside the blend P3HT:PCBM (1:1). The calculations were carried out using the FDTD software implementation from Lumerical, version 7.5.¹⁸ Data of the complex refractive index for the blend were taken from Monestier *et al.*¹⁹ The dielectric function for PEDOT:PSS and ITO was taken from Hoppe *et al.*²⁰ To describe the silver metal nanoparticle, Aluminum metal electrode and glass we used experimentally measured permittivity data under high vacuum.²¹ The nanoparticle shell was defined as a dielectric with $n = 1.5$. For parameterization of the material data, a multi-coefficient model as provided by the software is used. We implemented periodic boundary conditions in x and y direction. Perfectly matched layer (PML) boundary conditions were used at the top and bottom of the simulation volume. A mesh size of 0.5 – 1 nm was used in the vicinity of the metal nanoparticle. The amplitude of the electromagnetic field $|E|^2$ is calculated with and without silver nanoprism. Using the E-field data we calculated the volume integrated optical absorption $L(\omega) = \varpi \cdot \text{Im}(\epsilon) \int |E|^2 dV$ in a 35 nm blend film (in which V is the volume of the active layer). The absorption enhancement AE then results as the ratio of the optical absorption for a film with and without metal nanoparticle. We then define the spectrum integrated absorption enhancement IAE using the AM1.5G solar spectrum as follows:

$$\text{IAE} = \frac{\int L^{\text{NP}}(\lambda) I_{\text{AM1.5}}(\lambda) d\lambda}{\int L^{\text{bare}}(\lambda) I_{\text{AM1.5}}(\lambda) d\lambda} \quad (1)$$

where L^{NP} and L^{bare} are the optical absorption in the blend with and without nanoparticle, respectively. IAE is a measure for the enhancement that can be expected in terms of the devices' photocurrent.

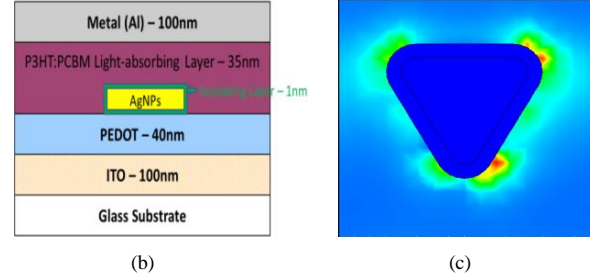
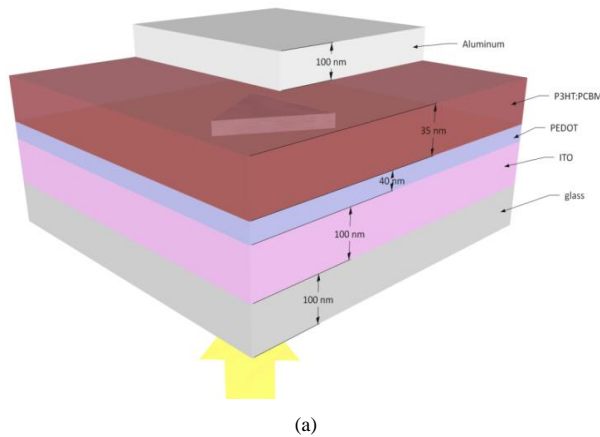


Figure 1. (a) Conventional structure of organic solar cell containing silver nano-prisms covered by 1-nm oxide; (b) side view; (c) top view of optical carrier generation rate in P3HT:PCBM layer in the presence of silver nano-prisms.

Next, we optimized the dimensions, i.e., thickness and edge length, of the AgNP based on the shape shown in Fig. 1, and which is representative of NPs typically observed in TEM micrographs, to give maximum IAE. In addition to the particle dimensions, we optimized the particle period/density. The IAE goes through a maximum when increasing the particle density and decreases for very high particle densities. For optimization of the particle size and period we applied the particle swarm optimization (PSO) algorithm provided by the Lumerical software. PSO is a nature-inspired stochastic evolutionary computation technique that has been successfully introduced in electromagnetic optimizations and other fields.^{17, 22} The PSO algorithm consists of 40 generations with each generation consisting of 20 simulations, where each simulation calculates the IAE for a specific set of parameters (a total of 800 simulations). Based on previous experimental work and experience,¹ the range of possible particle dimensions and periods were limited to: thickness: 5 – 15 nm, edge length: 5 – 50 nm, period: 150 – smallest possible edge length, which means that in the extreme case the particles are allowed to touch.

B. Optical optimization of device design

The normal device geometry adopted here consisted of the following layers: glass (100 nm) / ITO (100 nm) / PEDOT:PSS (40 nm) / AgNP/P3HT:PCBM (35 nm) / Al (100 nm). The maximum IAE was achieved with an AgNP with 8 nm edge length, 15 nm thickness and 17 nm period resulting in an overall absorption enhancement of 27% for unpolarized light within the wavelength range 300 – 800 nm. Note that the aspect ratio, i.e., edge length/height, of the optimized particle shape is very small (~0.5), while typically synthetic colloidal silver nanoprisms have aspect ratios > 2. The origin for this geometrical optimum is a balance between optical losses, including reflection and absorption due to the NP film, and the magnitude of plasmonic near field enhancement at a given spectral overlap between the absorption of the blend and the plasmon resonance of the particle. The in-plane dipole resonance of the optimized particle is at around 680 nm when embedded in the blend. By reducing the aspect ratio of the silver nanoprism the LSPR is shifted to the blue spectral region thereby increasing the spectral overlap and facilitating coupling of the plasmon resonance to excitation of the P3HT:PCBM blend.

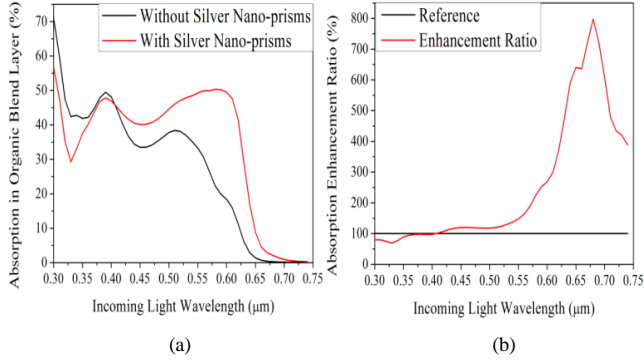


Figure 2. (a) Comparison of light absorption percentage in 35nm P3HT:PCBM layer as function of incoming light wavelength; (b) Enhancement of light absorption at the presence of silver nano-prisms.

III. DEVICE SIMULATION

A. Device calculation procedure

From the electronic device simulation point of view, the Poisson equation (with trap states):

$$\nabla^2 \Phi = -\frac{q(p-n+N_d^+-N_a^-)+\rho_{\text{trap}}}{\kappa\epsilon} \quad (2)$$

is coupled with the electron and hole continuity equations:

$$\begin{cases} \frac{\partial n}{\partial t} = \frac{1}{q} \nabla \cdot \vec{J}_n + G_n - R_n \\ \frac{\partial p}{\partial t} = -\frac{1}{q} \nabla \cdot \vec{J}_p + G_p - R_p \end{cases} \quad (3)$$

for inorganic semiconductor simulations, where Φ is the electrostatic potential, n and p are the electron and hole density, N_d^+ and N_a^- are concentration of ionized donors and acceptors, ρ_{trap} is the charge density contributed by traps, ϵ is electrical permittivity, \vec{J}_n and \vec{J}_p are electron and hole current density, G_n and G_p are electron/hole net generation rate, and R_n and R_p are electron/hole net recombination rate, respectively. For organic materials, the electrons and holes excited by incident light are initially bound together, forming excitons.²⁵⁻²⁵ Thus we apply singlet-exciton continuity equation to represent the behavior of excitons that can diffuse to the P3HT/PCBM interface and dissociate into electrons and holes:

$$\frac{\partial N_{\text{ex}}}{\partial t} = \nabla \cdot D_{\text{ex}} \nabla N_{\text{ex}} + G_{\text{ex}} - R_{\text{ex}} - \frac{N_{\text{ex}} - N_{\text{ex}}^{\text{equilibrium}}}{\tau} \quad (4)$$

where N_{ex} is the singlet exciton density, D_{ex} is the singlet exciton diffusion constant, G_{ex} is the carrier bimolecular recombination rate acting as a singlet exciton generation term, R_{ex} is the net singlet exciton recombination rate, and τ is the singlet exciton lifetime.

Electronic device simulations include Eqs. (2), (3) and (4) to simulate the electrical behavior of organic solar cells, while solving for electric field and electrostatic potential distribution inside the device to give device performance such as short-circuit current (Jsc), open-circuit voltage (Voc) and fill-factor (FF).

B. Enhancement of organic solar cells performance at the presence of silver nano-prisms

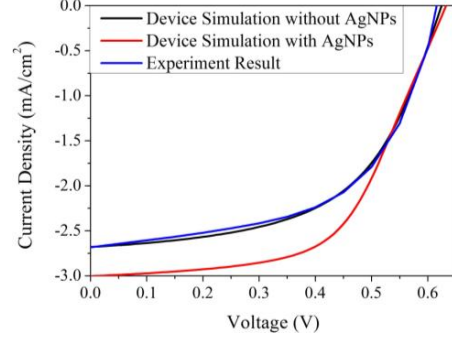


Figure 3. Current-Voltage plots for 35-nm conventional organic solar cells with / without the presence of silver nano-prisms.

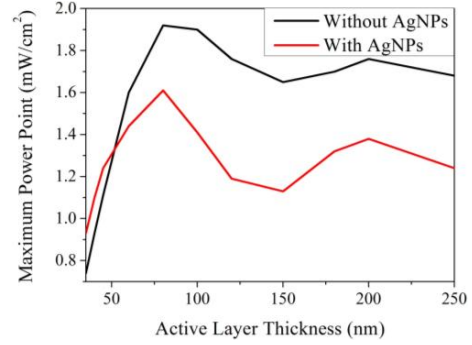


Figure 4. Maximum power point for 35-nm conventional organic photovoltaic devices with and without silver nano-prisms, at different thickness of P3HT:PCBM layer.

The current-voltage (I-V) plots for conventional organic photovoltaic (OPV) device at 1-sun, with and without silver nano-prisms are illustrated in Fig. 3. We first fit our model parameters for OPV without silver nano-prisms, including electron affinities of ITO, PEDOT, and Aluminum, as well as the HOMO/LUMO levels of P3HT:PCBM. After the fitting process, we then predict the I-V plot for OPV device at the presence of silver nano-prisms. It is clear from Fig. 3 that including silver nano-prisms inside the P3HT:PCBM layer will increase the current density without decreasing open-circuit voltage dramatically, thus increasing the overall maximum power density.

On the other hand, adding silver nano-prisms can only benefit the OPV device performance for ultra-thin (< 50 nm) layer of P3HT:PCBM, as illustrated in Fig. 4. For organic active layer thickness approaching ~ 180 nm, since nearly 99% of sunlight has already been absorbed in the active layer, adding silver nano-prisms actually hurt the device performance since they themselves absorbed some portion of incoming sunlight.

C. Impact from floating gate voltage

To further understand the device performance, we add gate contact at silver nano-prism / covering oxide interface. By keeping the gate voltage at a constant value, and sweeping the anode voltage at ITO from 0 to 0.8V, we get the I-V plots in

Fig. 5. The ill-shaped I-V curve at low gate voltage ($V_{\text{gate}} < 0.6\text{V}$) is due to the strong charge accumulation at the silver nano-prism / covering oxide interface, as illustrated in Table I.

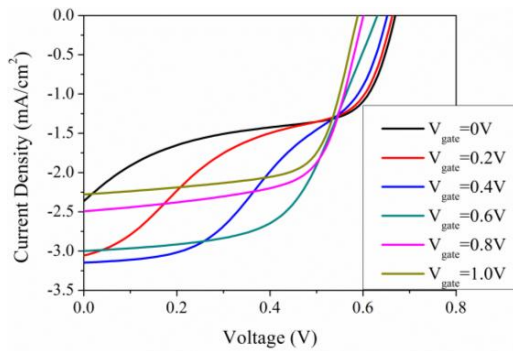


Figure 5. Current-Voltage plots for 35-nm conventional organic solar cells at the presence of silver nano-prisms, at different gate voltage.

TABLE I. OPV DEVICE PERFORMANCE AS FUNCTION OF APPLIED GATE VOLTAGE

V_{gate} V	J_{sc} mA/cm^2	V_{oc} V	P_{max} mW/cm^2	FF %
0	2.365	0.669	0.709	44.80
0.2	3.057	0.663	0.697	34.40
0.4	3.147	0.652	0.827	40.21
0.6	3.000	0.631	1.087	57.30
0.8	2.495	0.601	0.957	64.06
1.0	2.280	0.587	0.898	67.32

IV. SUMMARY

In summary, we established a simulation framework for modeling the optics and device behavior of organic solar cells at the presence of silver nano-prisms. Optics simulation optimizes the AgNPs structure design, and the resonance peaks are tunable via changing the size of AgNPs. Device simulation predicts $\sim 20\%$ enhancement in short-circuit current for ultra-thin (35nm) P3HT:PCBM light absorption layer. By tuning the applied gate voltage on the silver nano-prisms, the shape of I-V curve can be further modified to achieve better maximum power density.

REFERENCES

- [1] A. P. Kulkarni, K. M. Noone, K. Munechika, S. R. Guyer, and D. S. Ginger, "Plasmon-Enhanced Charge Carrier Generation in Organic Photovoltaic Films Using Silver Nanoprisms," *Nano. Lett.* vol. 10, pp. 1501-1505, 2010.
- [2] S. Karg, W. Riess, V. Dyakonov, and M. Schwoerer, "Electrical and optical characterization of poly(phenylene-vinylene) light emitting diodes," *Synth. Metals* vol. 54, pp. 427-433, 1993.
- [3] C. W. Tang, "Two-layer organic photovoltaics cell," *Appl. Phys. Lett.* vol. 48, pp. 183-185, 1986.

- [4] J. J. M. Halls, C. A. Walsh, N. C. Greenham, E. A. Marsaglia, R. H. Friend, S. C. Moratti, and A. B. Holmes, "Efficient photodiodes from interpenetrating polymer networks," *Nature* vol. 376, pp. 498-500, 2002.
- [5] S. Sista, Z. R. Hong, L. M. Chen, and Y. Yang, "Tandem polymer photovoltaic cells – current status, challenges and future outlook," *Energy Environ. Sci.* vol. 4, pp. 1606-1620, 2011.
- [6] M. A. Green, K. Emery, Y. Hishikawa, W. Warta, and E. D. Dunlop, "Solar cell efficiency tables (version 39)," *Prog. Photovolt: Res. Appl.* vol. 20, pp. 12-20, 2012.
- [7] F. J. Haug, T. Soederstroem, O. Cubero, V. Terrazzoni-Daudrix, and C. Ballif, "Plasmonic absorption in textured silver back reflectors of thin film solar cells," *J. Appl. Phys.* vol. 104, 064509 (2008).
- [8] F. C. Chen, and Y. K. Lin, "Submicron-scale manipulation of phase separation in organic solar cells," *Appl. Phys. Lett.* vol. 92, 023307 (2008).
- [9] W. L. Ma, C. Y. Yang, X. Gong, W. H. Lee, and A. J. Heeger, "Thermally stable, efficient polymer solar cells with nanoscale control of the interpenetrating network morphology," *Adv. Funct. Mater.* vol. 15, pp. 1617-1622, 2005.
- [10] L. M. Liu, W. E. Stanchina, and G. Y. Li, "Performance analysis of bulk heterojunction solar cells fabricated by polymer:fullerene:carbon-nanotube composites," *IEEE Nanotechnology Materials and Devices Conf. (NMDC '09)*, pp. 13-18, 2009.
- [11] Y. M. Liu, T. Zentgraf, G. Bartal, and X. Zhang, "Transformational plasmon optics," *Nano. Lett.* 10, pp. 1991-1997, 2010.
- [12] J. F. Torrado, J. B. Gonzalez-Diaz, M. U. Gonzalez, A. Garcia-Martin, and G. Armelles, "Magneto-optical effects in interacting localized and propagating surface plasmon modes," *Opt. Express* 18, pp. 15635-15642, 2010.
- [13] M. D. Arnold, and R. J. Blaikie, "Using surface-plasmon effects to improve process latitude in near-field optical lithography," *IEEE Nanoscience and Nanotechnology Conf. (ICONN '06)*, pp. 548-551, 2006.
- [14] K. Okamoto, I. Niki, A. Shvartser, Y. Narukawa, T. Mukai, and A. Scherer, "Surface-plasmon-enhanced light emitters based on InGaN quantum wells," *Nature Mater.* vol. 3, pp. 601-605, 2004.
- [15] S. Pillai, K. R. Catchpole, T. Trupke, and M. A. Green, "Surface plasmon enhanced silicon solar cells," *J. Appl. Phys.* vol. 101, 093105, 2007.
- [16] J. M. Li, W. F. Ma, C. Wei, J. Guo, J. Hu, and C.C. Wang, "Poly(styrene-co-acrylic acid) core and silver nanoparticle/silica shell composite microspheres as high performance surface-enhanced Raman spectroscopy (SERS) substrate and molecular barcode label," *J. Mater. Chem.* vol. 21, pp. 5992-5998, 2011.
- [17] G. X. Du, T. Mori, M. Suzuki, S. Saito, H. Fukuda, and M. Takahashi, "Evidence of localized surface plasmon enhanced magneto-optical effect in nanodisk array," *Appl. Phys. Lett.* vol. 96, 081915, 2010.
- [18] <http://www.lumerical.com>
- [19] F. Monestier, J. J. Simon, P. Torchio, L. Escoubas, F. Flory, S. Bailly, R. de Bettignies, S. Guillerez, and C. Defranoux, "Modeling the short-circuit current density of polymer solar cells based on P3HT:PCBM blend," *Sol. Energ. Mat. Sol. C.* vol. 91, pp. 405-410, 2007.
- [20] H. Hoppe, N. S. Sariciftci, and D. Meissner, "Optical constants of conjugated polymer/fullerene based bulk-heterojunction organic solar cells," *Mol. Cryst. Liquid Cryst.* vol. 385, pp. 113-119, 2002.
- [21] E. D. Palik, *Handbook of Optical Constants of Solids*, vol. 1. Academic Press: Orlando, 1985.
- [22] J. Robinson and Y. Rahmat-Samii, "Particle swarm optimization in Electromagnetics," *IEEE Trans. Antennas and Propagat.* vol. 52, pp. 397 – 407, 2004.